AIChE

Performance Features of Pt/BaO Lean NOx Trap with Hydrogen as Reductant

Robert D. Clayton, Michael P. Harold, and Vemuri Balakotaiah
Dept. of Chemical & Biomolecular Engineering, University of Houston, Houston, TX 77204

DOI 10.1002/aic.11710
Published online February 3, 2009 in Wiley InterScience (www.interscience.wiley.com).

The performance of a model Pt/BaO/Al_2O_3 monolith catalyst was studied using H_2 as the reductant. The dependence of product selectivities on operating parameters is reported, including the durations of regeneration and storage times, feed composition and temperature, and monolith temperature. The data are explained in terms of a phenomenological model factoring in the transport, kinetic, and spatio-temporal effects. The Pt/BaO catalyst exhibits high cycle-averaged NOx conversion above 100°C, generating a mixture of N_2 and byproducts NH_3 and N_2O. The cycle-averaged NOx conversion exhibits a maximum at about 300°C corresponding to the NOx storage maximum. The N_2 selectivity exhibits a maximum at a somewhat higher temperature, at which point the NH_3 selectivity exhibits a minimum. This trend conveys the intermediate role of NH_3 in reacting with stored NOx. Both N_2 and N_2O are also formed during the storage steps from the oxidation of NH_x species produced during the regeneration. © 2009 American Institute of Chemical Engineers *AIChE J,* 55: 687–700, 2009
Keywords: NOx, hydrogen, platinum, barium, selective catalytic reduction, NOx storage and reduction, lean NOx trap

Introduction

Lean burn and diesel vehicles have become increasingly attractive because of rising fuel costs. However, stringent demands on reducing nitrogen oxides (NO and NO_2; referred to as NOx) in the exhaust of lean burn and diesel vehicles have been mandated by the EPA. The development of the Lean NOx Trap (LNT) has been found to be a promising solution to reducing NOx emissions from these vehicles.[1–4] The LNT is a periodically operated, multi-functional adsorptive catalytic reactor that is operated by cycling between lean and rich conditions, which are referred to as the "storage" and "regeneration" steps. During the storage step, NOx produced during typical operation of a lean burn engine is "trapped" on the storage component of the catalyst (typically BaO). During the regeneration step, rich conditions are produced by either running the engine rich or injecting a reductant (such as fuel or reformed fuel) into the exhaust upstream of the LNT. Regeneration is accomplished on a highly-active precious metal (Pt or Pt/Rh). The duration of the lean and rich steps are of the order of 60–120 s and 1–10 s, respectively.

Different types of LNT designs and operating configurations are under development. The conventional LNT is intended to maximize the conversion of exhaust NOx to N_2. NH_3 is an undesired byproduct in the conventional LNT. On the other hand, a LNT coupled with selective catalytic reduction (SCR) should produce NH_3, which is trapped downstream in the SCR and selectively reduces NOx. The LNT may be exposed to quite different feed conditions depending on the nature of the reductant (H_2, CO, low or high molecular weight hydrocarbons) and the way the reductant is generated. For example, the level of O_2 present during the regeneration may be between 0 and a few percent. The latter may occur in diesel applications in which fuel is injected into the exhaust directly or designs in which the diesel oxidation catalyst (DOC) is positioned upstream of the LNT. In such cases, the rich feed to the LNT will have little O_2. Therefore, both anaerobic and aerobic regeneration feeds have been studied. Understanding the LNT is more difficult for aerobic

Correspondence concerning this article should be addressed to M. P. Harold at mharold@uh.edu or V. Balakotaiah at bala@uh.edu.

Table 1. Catalysts Used and Their Properties

Sample	Pt (wt %)	BaO (wt %)	Pt Dispersion (%)	Pt Area (m^2/g)	Pt Particle Size (nm)	BET Area (m^2/g)
B2	1.27	16.5	33	1.04	3.43	109
B3	2.2	16.3	21.9	1.19	5.18	116
A3	2.63	0	20.3	2.21	5.59	–

regenerations[5–9] due to the large exotherm created by the oxidation of the reductant. Nearly isothermal regenerations (anaerobic and long duration) may be unrealistic but simplify the interpretation of data.

The effectiveness of different types of reductants such as propylene, CO, H_2, and NH_3 has been compared by many groups.[5,10–14] H_2 has been found to be the most effective reductant, especially at low temperatures (<250°C).[5,10,11] The reaction of NOx and H_2 can produce a complex mixture of N_2, N_2O, and NH_3. As mentioned, the production of ammonia is undesirable in conventional LNT systems but is desirable in LNT/SCR hybrid systems.[15]

Little attention has been given to low temperature (< 200°C) operation of the LNT.[5,16,17] These conditions are encountered in the exhaust of lean burn and diesel vehicles during the so-called "cold-start." Understanding the low temperature performance of the LNT is especially important for vehicles that are only driven a short distance (insufficient time for engine/exhaust to heat up). Ramanathan et al.[18] used a transient one-dimensional two-phase model to obtain an explicit light-off criterion that was used to predict the nature of ignition (front-end, middle, or back-end) in catalytic converters (TWC), to minimize cold-start emissions. Similar developments are needed for the more complex LNT, but the measurement of comprehensive performance data are critical, which is the motivation for this study.

The objective of this study is to elucidate the performance of a model $Pt/BaO/Al_2O_3$ lean NOx trap using H_2 as the reductant. This is accomplished by determining the effects of catalyst temperature, rich feed composition (NO, H_2, and O_2), duration of the lean and rich steps, and the reductant to stored NOx ratio on the cycle-averaged conversions and selectivities. A phenomenological model of the LNT building off of recent literature developments is utilized to help explain some of the experimental trends.

Experimental

Catalyst samples

The catalyst samples used for these experiments were monolith catalysts provided by BASF Catalysts LLC (Iselin, New Jersey). Larger cylindrical cores (D = 3.8 cm, L = 7.6 cm) were cut using a dry diamond saw to smaller, nearly cylindrical shapes ($D \sim$ 0.8 cm, L = 2 cm). The samples contained varied amounts of Pt and BaO on a γ-alumina washcoat support adsorbed on a cordierite structure (~62 channels/cm^2). The mass of washcoat material (m_{wc}) on each monolith piece was ~110 mg. The compositions and properties of the catalysts are given in Table 1. The methods used to measure catalyst properties were described in a previous publication.[19] The monoliths were then wrapped in Fiberfrax® ceramic paper that had been heat treated and then placed in a quartz tube flow reactor.

Flow reactor set-up

The experimental set-up is the same as the one described in detail in a previous study.[19] A quadrupole mass spectrometer (MKS Spectra Products; Cirrus LM99) was added to the set-up during the course of this investigation. The QMS was tied into the effluent line ~0.7 m downstream of a FTIR. The QMS was calibrated for all of the reactants and products, but was only used to monitor N_2 in this study, enabling the closure of the N balance. In those particular experiments, Argon was used as the diluent; otherwise, N_2 was the diluent. The time delays for the QMS and FTIR were accounted for in the concentration vs. time plots by shifting the data corresponding to their respective time delays as estimated by inert pulsing experiments.[20] However, some dispersion was observed to occur in the effluent lines, slightly affecting the concentration profiles.[6] Temperatures were monitored with three K-type stainless steel sheathed thermocouples. One thermocouple (0.02 inches o.d.) was used to measure the monolith temperature (T_m) and was positioned within an internal monolith channel at the approximate mid-point of the monolith (radial and axial). The second and third thermocouples (0.033 inch o.d.) monitored the gas feed (T_f) and outlet (T_0) temperatures about 1 cm upstream and downstream of the catalyst, respectively.

NO storage experiments

Prior to the storage experiments, a conditioning process was imposed to maximize reproducibility from run to run over the course of the study. This procedure included a minimum of 15 cycles of alternating lean and rich feeds until a cyclic steady-state was reached at the particular inert feed temperature of the storage experiment. Following Kabin et al.,[21] the inert feed temperature is the feed gas temperature to the reactor under nonreactive conditions; N_2 or Ar only. The lean feed had a 60-s duration and contained 500 ppm NO and 5% O_2, whereas the rich feed was 10 s long and contained 0.5% O_2 and 2% H_2. Storage data obtained during this cycling protocol are more relevant to actual operation than on a completely reduced catalyst. For example, the NO_x trap is not completely regenerated during cycling. After this conditioning procedure, Ar was flowed over the catalyst for 5 min to cool the monolith down to the desired inert feed temperature to ensure that the monolith temperature was constant throughout the ca. 300 s storage experiment. The total NOx stored (moles/g washcoat) was calculated by

$$NO_X^{stored}(t_s) = \frac{\int_0^{t_S} \left[F_{NO}^0 - F_{NOx}(t)\right] dt}{m_{w.c.}} \quad (1)$$

Equation 1 will slightly over-estimate the amount of NOx stored at low temperatures as discussed later.

Lean and rich cycling experiments

A base case cycling experiment was defined to compare experimental reproducibility and to asses catalyst activity. Unless otherwise stated, the total cycle time was 70 s, with 10 s rich and 60 s lean. The storage step of the base case experiment comprised a feed containing 500 ppm NO and 5% O_2 in N_2, while the rich pulse contained 5.1% H_2, 1.5% O_2, and 500 ppm NO in N_2 at a total flow rate of 1000 sccm (GHSV = 60,000 h^{-1}). The composition corresponded to a pulse stoichiometric number ($S_{N,p}$) of 0.6 where $S_{N,p}$ = $(2[O_2] + [NO])/[H_2]$. The excess H_2 was 2.05% (excess H_2 = $[H_2]$–$2[O_2]$–$[NO]$), assuming all of the O_2 and NO in the rich pulse reacts with H_2 to form H_2O and N_2. The relatively low O_2 concentration in the rich pulse corresponds to the case when reductant is added to the exhaust gas or incomplete O_2 consumption occurs during the rich combustion in the engine. The cycle-averaged results were obtained over at least five cycles after the system had reached a cyclic steady-state. The cycle-averaged NOx and H_2 conversions were calculated by

$$X_{NOx} = \frac{\int_0^{t_{S+R}} \left[F^0_{NO}(t) - F_{NOx}(t)\right]\, dt}{\int_0^{t_{S+R}} F^0_{NO}(t)\, dt} \tag{2a}$$

$$X_{H_2} = \frac{\int_0^{t_{S+R}} \left[F^0_{H_2}(t) - F_{H_2}(t)\right]\, dt}{\int_0^{t_{S+R}} F^0_{H_2}(t)\, dt} = \frac{\int_0^{t_{S+R}} \left[F_{H_2O}(t) + 1.5F_{NH_3}(t)\right]\, dt}{\int_0^{t_{S+R}} F^0_{H_2}(t)\, dt} \tag{2b}$$

The cycle-averaged NH_3, N_2, and N_2O selectivities are defined as

$$S_{NH_3} = \frac{\int_0^{t_{S+R}} F_{NH_3}(t)\, dt}{\int_0^{t_{S+R}} \left[F^0_{NO}(t) - F_{NOx}(t)\right]\, dt} \tag{3a}$$

$$S_{N_2} = \frac{2\int_0^{t_{S+R}} F_{N_2}(t)\, dt}{\int_0^{t_{S+R}} \left[F^0_{NO}(t) - F_{NOx}(t)\right]\, dt} \tag{3b}$$

$$S_{N_2O} = \frac{2\int_0^{t_{S+R}} F_{N_2O}(t)\, dt}{\int_0^{t_{S+R}} \left[F^0_{NO}(t) - F_{NOx}(t)\right]\, dt} \tag{3c}$$

Activity changes were minimized by ensuring that the catalyst temperature did not exceed 450°C for an extended period.

Experiments were carried out in which the lean and rich step durations were varied with different rich pulse compositions to determine optimal operation conditions; that is, conditions that give high NOx and reductant conversion. The storage time was varied from 5 to 150 s, while the regeneration was varied from 1 to 20 s for the cyclic steady-state experiments. The rich pulse timing was also varied for a fixed amount of NOx stored. This was done because at a cyclic steady-state, with varied regeneration timing, the amount of stored NOx will be different for each of the experiments. The "rich pulse" composition was varied over a range spanning excessively rich to slightly lean ($0.4 < S_{N,p} < 1.15$). This was done by varying the feed H_2 for a fixed O_2 feed rate. Very rich pulse conditions were also studied to focus on NH_3 formation and reaction. Experiments were also carried out with and without NO in the rich pulse to determine the effect of gas phase NO. During actual operation, NO flows continuously, so these experiments provide a way to compare conversion and selectivity effects of gas phase NO.

Experimental Results

NOx storage

Storage experiments were carried out over a range of temperatures and storage times to quantify the amount of NOx stored as a function of these variables on both Pt/Al_2O_3 and $Pt/BaO/Al_2O_3$ monoliths. Figure 1a has storage trends that are similar to results reported previously for $Pt/BaO/Al_2O_3$.[8,21] At a storage time of 60 s, a broad maximum was observed that spanned the temperature range of 240–400°C. Kabin et al.[21] also observed this broad maximum in NOx storage for fresh and aged Pt/BaO catalysts. At longer exposure times (exceeding 5 min), the high temperature maximum narrowed and the amount of NOx stored increased. The storage data at lower temperature has a second local maximum for

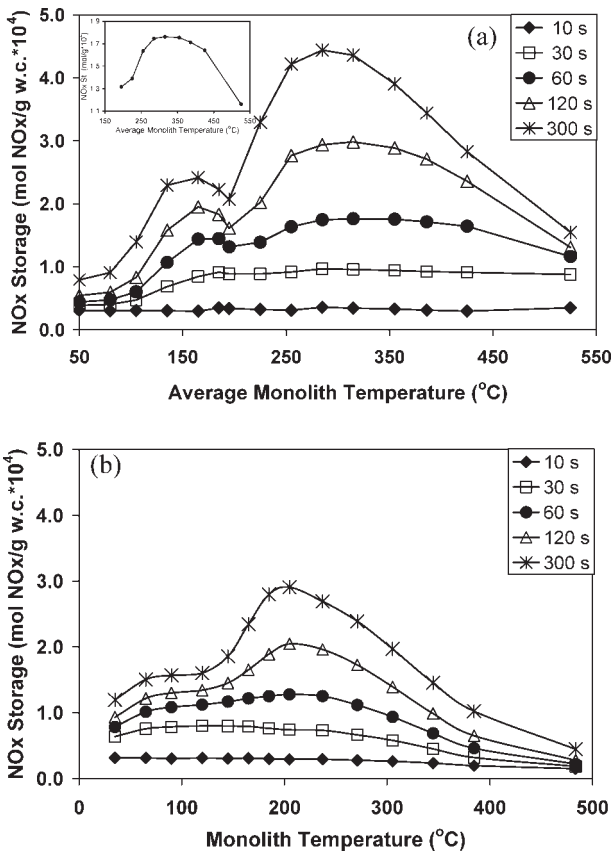

Figure 1. NOx storage as a function of monolith temperature.

(a) varied storage time on catalyst B3 (Pt/BaO) (b) varied storage time on catalyst A3 (Pt only); (500 ppm NO and 5% O_2, balance N_2).

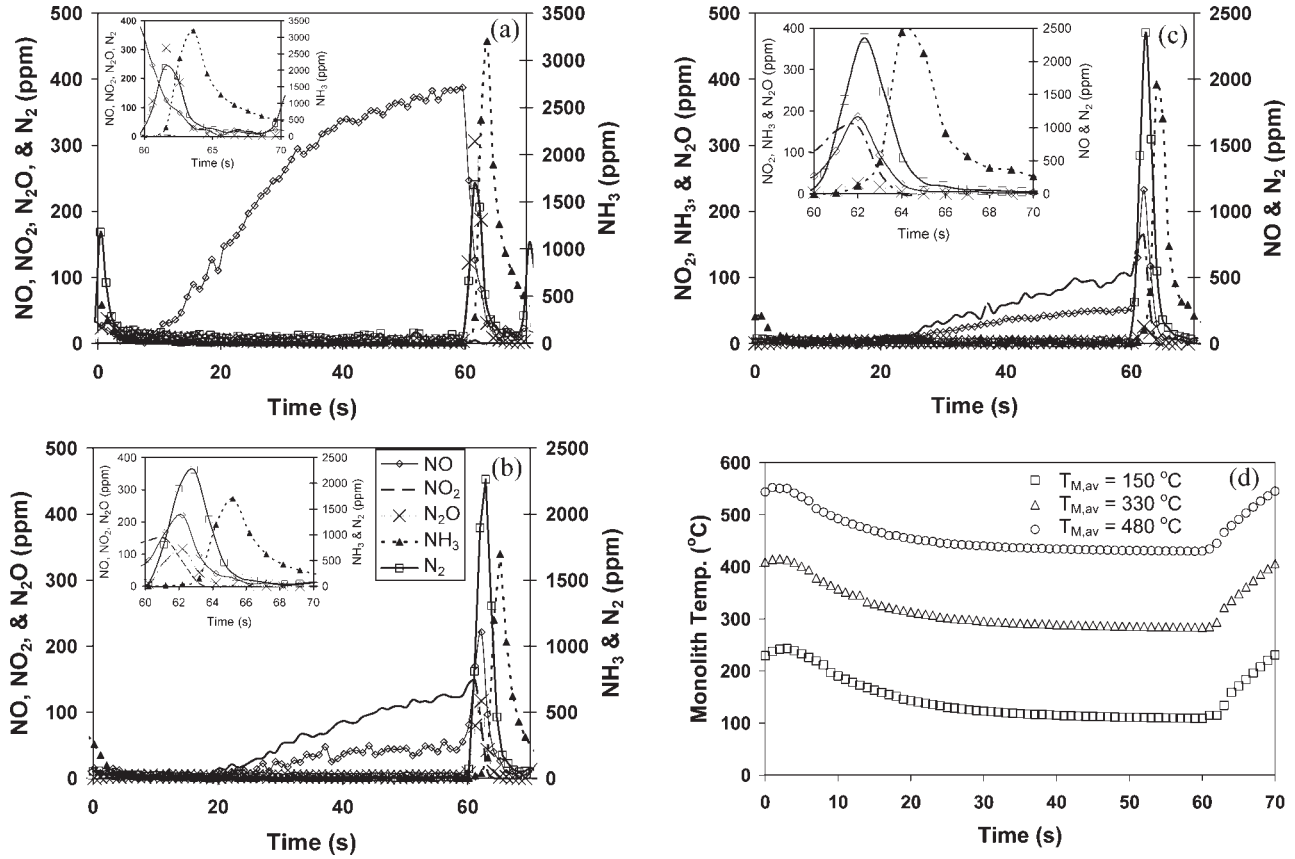

Figure 2. Cycling effluent concentrations for catalyst B2 at (a) 150°C; (b) 330°C (c) 480°C; (d) corresponding monolith temperature profiles.

(Lean: 500 ppm NO, 5% O_2, balance Ar (60 s); Rich: 1.5% O_2, 5.1% H_2, balance Ar (10 s) and $S_{N,p} = 0.6$). The legend in (b) applies to (a)–(c).

storage durations exceeding 60 s. The existence of two maxima was previously reported by Muncrief et al.[8] for Pt/BaO/Al_2O_3 powder. NOx storage on Pt/Al_2O_3 monolith was also studied to determine the contribution of the Al_2O_3 support (Figure 1b). The Pt/Al_2O_3 monolith was less effective than the Pt/BaO/Al_2O_3 monolith in NOx storage at higher temperatures. The Pt/Al_2O_3 exhibited only one NOx storage maximum at about 200°C.

Storage-regeneration cycling

In Figure 2, the transient outlet concentration profiles for N_2, N_2O, NH_3, NO, and NO_2 are shown for a typical set of lean-rich cycling experiments at low (150°C), moderate (330°C), and high (480°C) temperature. In these experiments, the rich pulse was devoid of NO, while the 60-s lean and 10-s rich feeds had the following compositions: Lean: 500 ppm NO, 5% O_2, balance Ar; Rich: 1.5% O_2, 5.1% H_2, balance Ar. At 150°C, two peaks in N_2 and N_2O were observed, one at the onset of the rich pulse and the other at the beginning of the storage step (Figure 2a). The N_2O peak during the rich step decreased with increasing temperature for the three temperatures reported. This trend has been previously reported by Lindholm et al.[22] At all three temperatures, N_2 and N_2O were observed exiting the reactor just as the rich pulse was introduced, with NH_3 exiting the reactor last. The N_2O peak coincided with the "NOx puff," followed immediately by the N_2 peak, and then finally the NH_3 peak.

The corresponding transient monolith temperature profiles are shown in Figure 2d. At the onset of the reduction a large temperature rise was observed, due to the Pt-catalyzed oxidation of H_2. The temperature slowly decreased during the storage step. The temperature rise was about 120°C, measured at the midpoint of the monolith and was essentially independent of the feed temperature. Clayton et al.[5] recently showed that the temperature rise is highest at the front of the monolith (~160°C) under similar feed concentrations due to the majority of H_2 oxidation occurring there. Theis and Gulari[23] inferred the temperature of the precious metal sites to be 130°C higher than that of the exhaust gas exiting the LNT. Therefore, measuring the temperature inside a monolith channel does not give the actual temperature of the precious metal sites at which the reactions occur.

Cycle-averaged NOx conversion and product selectivities are reported in Figures 3a and 4a as a function of the cycle-averaged monolith temperature for the Pt/BaO/Al_2O_3 catalyst (B3). Two sets of rich pulse compositions are compared for a fixed O_2 concentration (1.5% O_2): 5.1% H_2 ($S_{N,p} = 0.6$) in Figure 3a and 3.8% H_2 ($S_{N,p} = 0.8$) in Figure 4a. These results revealed NOx conversion and N_2 selectivity exceeding

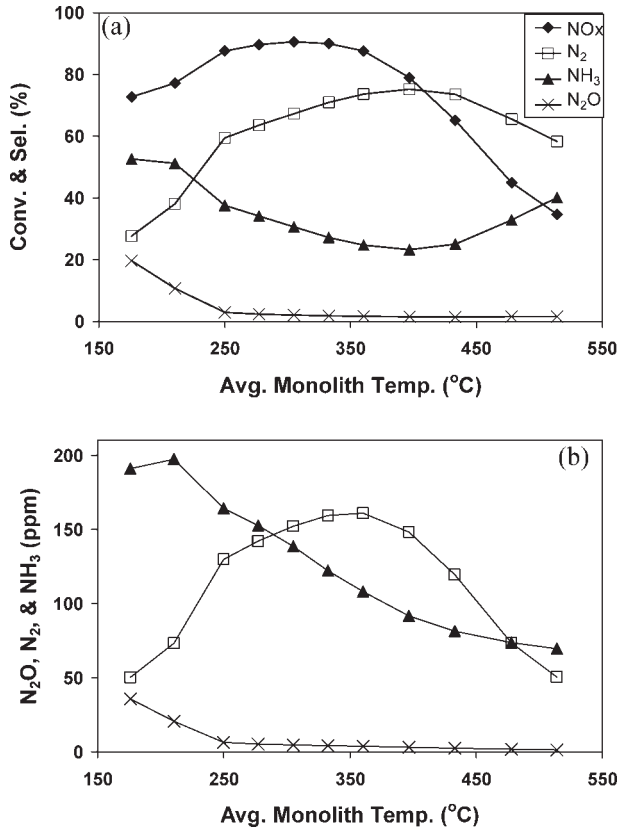

Figure 3. Time-averaged results as a function of temperature for catalyst B3.

(a) conversion and selectivities; (b) effluent concentrations of products; (Lean: 500 ppm NO, 5% O_2, balance N_2 (60 s); Rich: 500 ppm NO, 1.5% O_2, 5.1% H_2 ($S_{N,P}$ = 0.6), balance N_2 (10 s)). The legend applies to both figures.

80 and 60%, respectively, over moderate but different ranges of monolith temperature; the NOx conversion exceeded 80% between 250–360°C, while the N_2 selectivity exceeded 60% between 250–450°C. During the regeneration, the NH_3 selectivity exceeded 40% at low (<270°C) and high temperature (>450°C), with a broad minimum between those extremes. In contrast, the N_2O selectivity was negligible above 220°C. For this reason, the NH_3 selectivity trend was nearly the exact opposite of the N_2 selectivity (i.e., no other N-containing products were observed).

In Figures 3b and 4b, the cycle-averaged N_2, N_2O, and NH_3 concentrations are reported as a function of the cycle-averaged monolith temperature. The yield of N_2 exhibited a maximum at about 350°C for both the $S_{N,p}$ = 0.6 and 0.8 rich pulses. The yields of NH_3 and N_2O produced from the richer pulse ($S_{N,p}$ = 0.6) achieved a maximum at the lowest temperatures (ca. 200°C) and monotonically decreased with increasing temperature (Figure 3b). Similarly, for the "weaker" rich pulse ($S_{N,p}$ = 0.8), the yield of NH_3 decreased with increasing temperature with a small local maximum at about 430°C.

The effect of the amount of NOx stored on the regeneration of the NOx trap was studied by varying the storage time. In this set of cycling experiments shown in Figures 5 and 6, the anaerobic rich pulse composition was fixed at 2% H_2 for 10 s. With the pulse devoid of O_2, (2% H_2 in inert) nonisothermal effects were minimal (ΔT_m ~10–20°C). The duration of the storage step was varied from 5 to 150 s while maintaining a constant feed temperature (T_f = 295°C). Figure 5 shows the transient effluent concentrations of NH_3 (5a), N_2O (5b), and total NOx (5c). Ammonia appeared after a delay, the duration of which increased with increased NOx storage. Each experiment led to a maximum in the ammonia concentration prior to the end of the regeneration, and the maximum value increased with the storage duration. For the shortest storage times (5 and 10 s), NH_3 was detected in the effluent at about 2 s with its concentration peaking at about 180 and 500 ppm, respectively. Further increase in the storage time led to a monotonic increase in the delay breakthrough time of ammonia, the peak NH_3 concentration, and the time at which the peak ammonia occurred. The maximum ammonia concentration observed for this set of conditions was about 1650 ppm for the storage time of 150 s. On the other hand, the N_2O outlet concentration, shown in Figure 5b, increased as the storage time was increased up to 60 s. Beyond this storage time, the N_2O profiles remained nearly identical. In Figure 5c, the unreacted NOx concentration increased with storage time. For storage times shorter than 10 s, negligible NOx was observed.

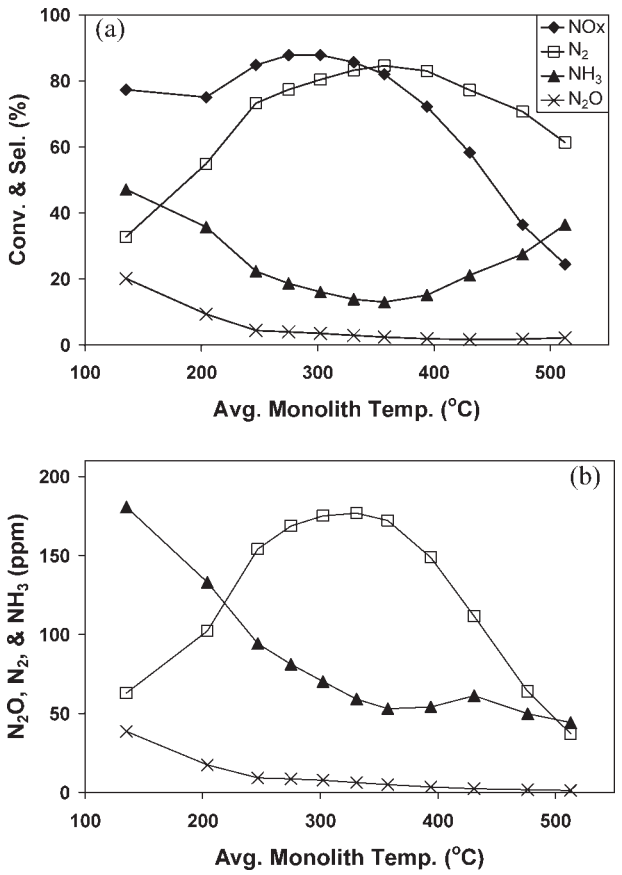

Figure 4. Time-averaged results as a function of temperature for catalyst B3.

(a) conversion and selectivities; (b) effluent concentrations of products; (Lean: 500 ppm NO, 5% O_2, balance N_2 (60 s); Rich: 500 ppm NO, 1.5% O_2, 3.8% H_2 ($S_{N,P}$ = 0.8), balance N_2 (10 s)). The legend applies to both figures.

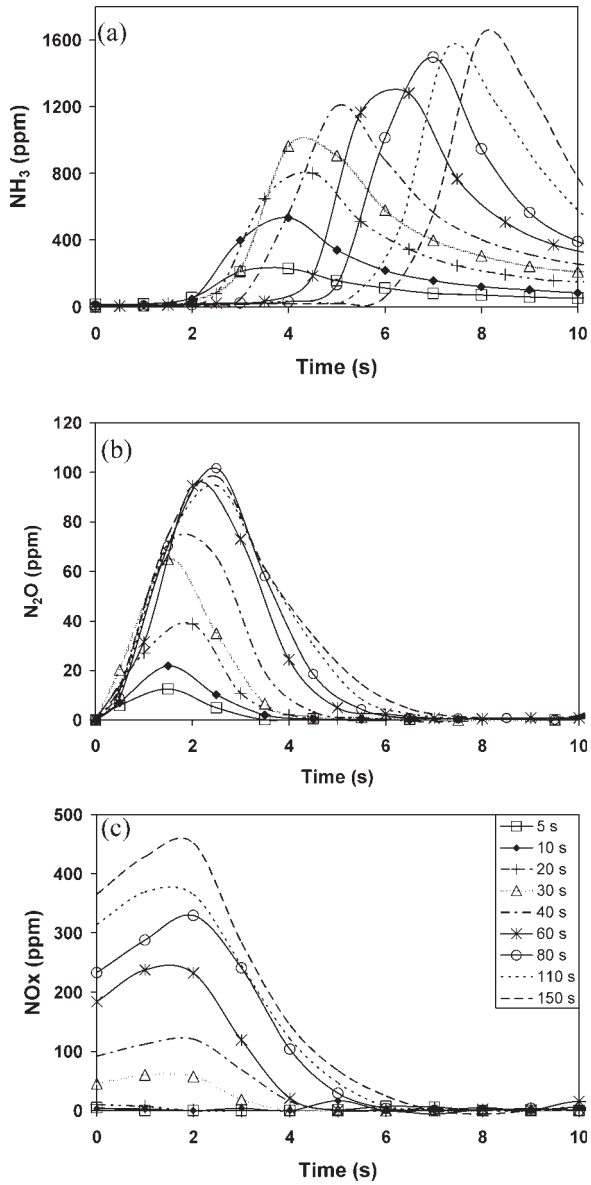

Figure 5. Cycling experiments for varied storage time on catalyst B3 at $T_{M,avg}$ = 295°C.

(a) effluent NH_3 concentration; (b) effluent N_2O concentration; (c) effluent NOx concentration; (Lean: 500 ppm NO, 5% O_2, balance N_2 (varied time); Rich: 2% H_2, balance N_2 (10 s)). The legend applies to all three figures.

From these data in Figure 5, cycle-averaged performance variables were determined. Figure 6a shows the dependence of the cycle-averaged NOx and H_2 conversions and product selectivities (N_2, N_2O, NH_3) on the duration of the storage step. Figure 6b shows the dependence of the yield (in moles) of nitrogen-based products formed as a function of the moles of NOx stored during the storage step. The cycle-averaged H_2 conversion and N_2 selectivity were determined by overall N and H balances. The cycle-averaged NOx conversion decreased monotonically with storage time, whereas the H_2 conversion increased. The conversions intersected at about 68% for a lean time of 110 s. With increasing storage time, the N_2 selectivity increased and the NH_3 selectivity decreased, whereas the N_2O selectivity remained at a nearly constant low level (Figure 6a). As shown in Figure 6b, the measured NH_3 and (estimated) N_2 yields both increased with increasing storage time until the total amount of stored NOx reached a critical value. This occurred at 110 s of storage (ca. 3.2×10^{-5} mol NOx) at which point the amount of NH_3 in the effluent began to decrease. Similar yield trends were observed for an aerobic rich pulses containing the same

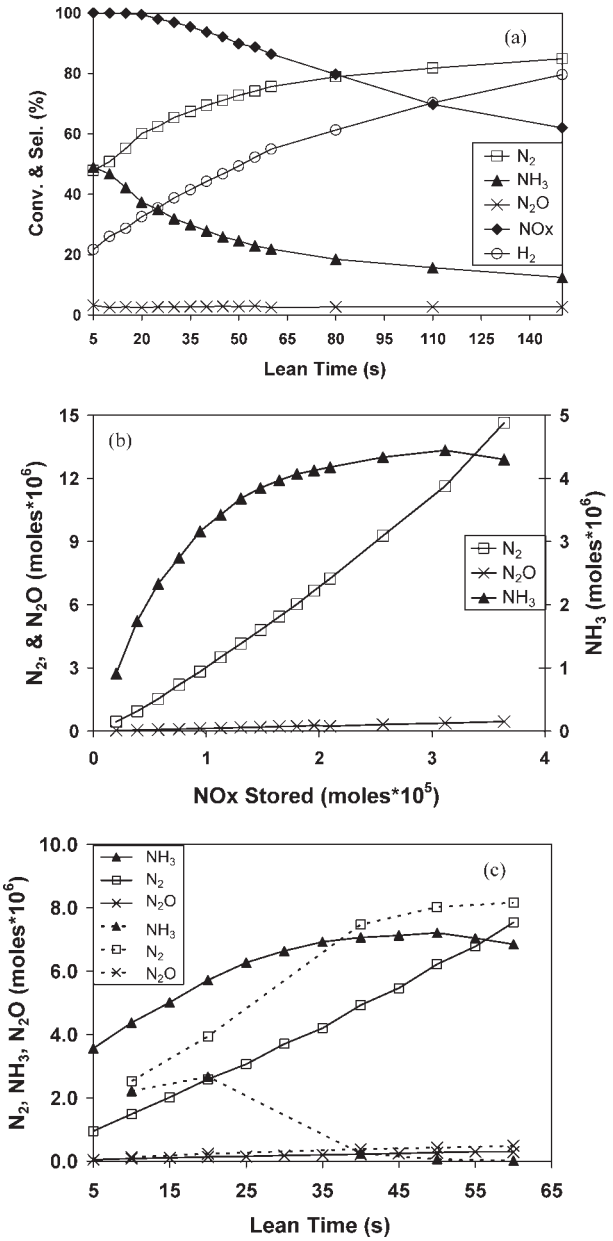

Figure 6. Time-averaged cycling results for varied storage time on catalyst B3 at $T_{M,avg}$ = 295°C.

(a) NOx and H_2 conversion and NH_3, N_2O, and N_2 selectivities (Rich: 2% H_2, balance N_2 (10 s)); (b) effluent concentrations of N_2, N_2O, and NH_3 (Rich: 2% H_2, balance N_2 (10 s)); (c) effluent concentrations of N_2, N_2O, and NH_3 (Rich: 500 ppm NO, 1.5% O_2, (—) 3.34% H_2 ($S_{N,p}$ = 0.9) and (—) 5.1% H_2 ($S_{N,p}$ = 0.6), balance N_2, (10 s)); (Lean: 500 ppm NO, 5% O_2, balance N_2 (varied time)).

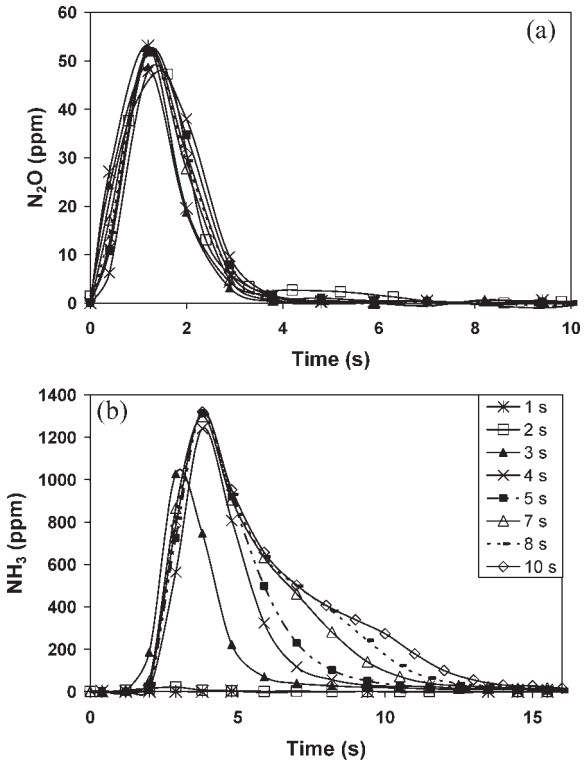

Figure 7. Cycling experiments for varied rich time on catalyst B3 at T_f = 290°C.

(a) effluent NH_3 concentration; (b) effluent N_2O concentration; (Lean: 500 ppm NO, 5% O_2, balance N_2 (60 s); Rich: 1.5% O_2, 5.1% H_2, balance N_2 (varied time) and $S_{N,P}$ = 0.6). The legend applies to both figures.

amount of excess H_2 (2%) as the feed concentration for the anaerobic pulse. For comparison, the results for a rich pulse containing considerably less excess H_2 (0.29%) are also shown in Figure 6c. The rich pulse contained 500 ppm NO, 1.5% O_2, and either 5.1% H_2 ($S_{N,p}$ = 0.6) or 3.34% H_2 ($S_{N,p}$ = 0.9). The duration of the step cycle (NOx storage value) at which the maximum in the effluent NH_3 concentration occurred decreased as the H_2 concentration was decreased from 5.1 to 3.34%. The corresponding effluent NH_3 outlet concentration approached zero as the ratio of the amount of H_2 fed in the pulse to the amount of stored NOx decreased.

The effect of the duration of the rich pulse on the effluent concentrations of products NH_3 and N_2O at a fixed feed temperature (290°C) are shown in Figure 7. For this set of experiments, the rich pulse contained 1.5% O_2 and 5.1% H_2 (aerobic regeneration, $S_{N,p}$ = 0.6) and its duration was varied from 1 to 10 s. This was accomplished first by completely regenerating the trap. Then an inert feed of N_2 was fed to the reactor prior to each of the storage experiments, and again after the 60 s storage. After which, the regeneration feed (of variable duration) was then directed to the reader, followed by a N_2, purge. The stored NOx in this set of experiments were within 2% of each other, enabling meaningful comparisons to be made. Thus, the relative ratio of excess reductant (H_2) to stored NOx varied systematically according to the duration of the rich pulse.

The N_2O concentration was observed to be independent of the rich pulse duration (Figure 7a). This indicates that the H_2 fed during the first second of the pulse was responsible for all of the N_2O produced. The results obtained for the ammonia were more complex. The NH_3 was not observed in the effluent for rich pulses that had durations less than 2 s. For pulses of durations 3 s or longer, the NH_3 concentration exhibited a maximum. The 3 s pulse duration resulted in a peak ammonia concentration of about 1000 ppm. For the pulses exceeding 4 s in duration, there was little change in the peak ammonia concentration (about 1300 ppm), or the time at which the peak occurred (about 5 s). The existence of a maximum in the ammonia is the net result of its formation, from reaction of H_2 and stored NOx, and its consumption, from reaction of NH_3 with stored NOx and/or O_2. After the maximum in NH_3 occurred, the tail of the NH_3 effluent curves decreased more gradually as the pulse duration increased. In fact, once the pulse was stopped, only N_2 flowed over the catalyst but NH_3 was still observed in the effluent.

The effect of the rich pulse duration on the cycle-averaged H_2 and NOx conversions is shown in Figure 8. In these experiments, the aerobic rich pulse contained a mixture of O_2 (1.5%) and H_2 (5.1%). These aerobic pulses introduced some temperature rise in the monolith, as described earlier in the context of Figure 2. For this set of experiments, the inert gas feed temperature was fixed ($T_{f,inert}$ = 280°C). One experimental condition ($S_{N,p}$ = 0.6, t_R = 3 s) was repeated after both sets of experiments were completed to assess the reproducibility and check for any catalyst deactivation. The NOx conversion decreased less than 1% (within experimental error), and the selectivities were nearly identical.

As seen in Figure 8 ($S_{N,p}$ = 0.6, 2.1% of excess H_2), for a pulse duration less than 3 s, the H_2 conversion was 100%. As the duration of the rich pulse was increased, the H_2 conversion decreased and approached 60% for long pulse times. This is merely a reflection of the rich pulse composition and reaction stoichiometry; that is, $S_{N,p}$*100% = 60%. The NOx conversion increased with increasing rich time for all rich

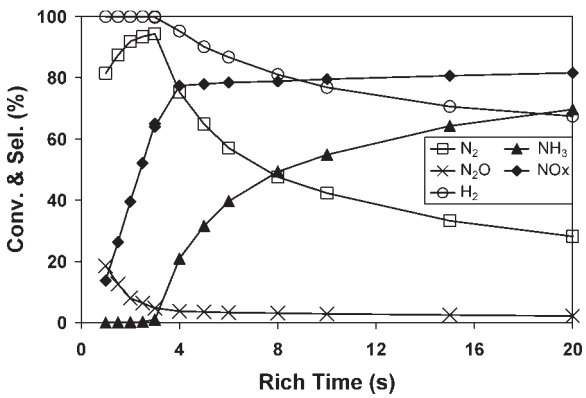

Figure 8. Cycle-averaged conversions and selectivities for varied rich cycle time on catalyst B2 at $T_{g,inert}$ = 280°C ($S_{N,p}$ = 0.6).

(Lean: 500 ppm NO, 5% O_2, balance Ar (60 s); Rich: 1.5% O_2, 500 ppm NO, 5.1% H_2, balance Ar (varied time)].

times studied. From a pulse time of 1 to 4 s, the NOx conversion increased sharply from about 15 to 78%. As the pulse time was further increased from 4 to 20 s, the NOx conversion approached an asymptotic value of about 82%. Pulses shorter than 4 s in duration were insufficient to regenerate the catalyst. An important finding from these experiments was the existence of an "optimal" rich pulse duration in which the H_2 and NOx conversions and N_2 selectivity achieved high values with a minimal duration of the rich pulse, or equivalently, amount of H_2 fed. This occurred for a pulse of between 3 and 4 s in duration, resulting in a N_2 selectivity of slightly over 90%, H_2 conversion of nearly 100%, and a NOx conversion of about 75%.

To determine the effects of gas phase NO during the rich pulse, a systematic comparison was made between rich pulse feeds containing NO (500 ppm) and ones devoid of NO. Figure 9 reports cycle-averaged effluent concentrations (N_2O, N_2, and NH_3) as a function of the cycle-averaged monolith temperature for three different aerobic (1.5% O_2) pulse feed compositions: $S_{N,p}$ = 0.6 (Figure 9a); 0.8 (Figure 9b); 0.9 (Figure 9c). A comparison of the pulses with and without NO clearly reveals a difference in the reaction of H_2 with stored NOx and with gas phase NO. The data show that for the richest pulse ($S_{N,p}$ = 0.6) devoid of NO, the regeneration produced approximately 2–6 ppm less N_2 and 59–68 ppm less NH_3 compared to the pulse containing NO over the temperature range studied (150–450°C). For the leaner pulses ($S_{N,p}$ = 0.8, 0.9), the effect of the added NO during the pulse resulted in the near convergence of the cycle-averaged NH_3 effluent concentrations from 150 to 270°C. On the other hand, the difference in the amount of N_2 produced generally increased with temperature for the leaner pulses. For all the three pulses, the difference in N_2O produced with and without NO fed during the regeneration was minimal except at the lowest temperature (150°C) and leanest pulse ($S_{N,p}$ = 0.9); in that case the N_2O concentration doubled when 500 ppm NO was added. At low temperatures (150°C), the difference in the amount of NH_3 formed from a rich pulse with and without NO was maximized for the three $S_{N,p}$ pulses.

The production of N_2 and N_2O are not confined to the regeneration step as seen in Figure 2a. A series of experiments were carried out to quantify the production of N_2 and N_2O during the lean storage step. Figure 10a shows the effluent profiles of N_2 and N_2O at 45 and 155°C whereas Figure 10b shows the moles of N_2 and N_2O formed during the lean and rich parts of the cycle. The rich pulse contained 2% H_2 and 0.5% O_2 for a wide range of temperatures. The formation of N_2O during the storage step decreased with increasing temperature from 45 to 300°C at which point N_2O was no longer detected. The amount of N_2 formed during the storage initially increased from 45 to 175°C. With further increase in the temperature, the production of N_2 decreased. On the other hand, the production of N_2 during the regeneration step slowly increased with temperature from 45 to 190°C, at which point a sharp increase in the production of N_2 occurred as the temperature was further increased. The production of N_2O during the regeneration was maximized at 175°C. The percent of N_2 and N_2O formed during the lean and rich are reported in Table 2, and the results show that at low temperatures (<110°C), the majority of N_2 and N_2O formation occur during the storage.

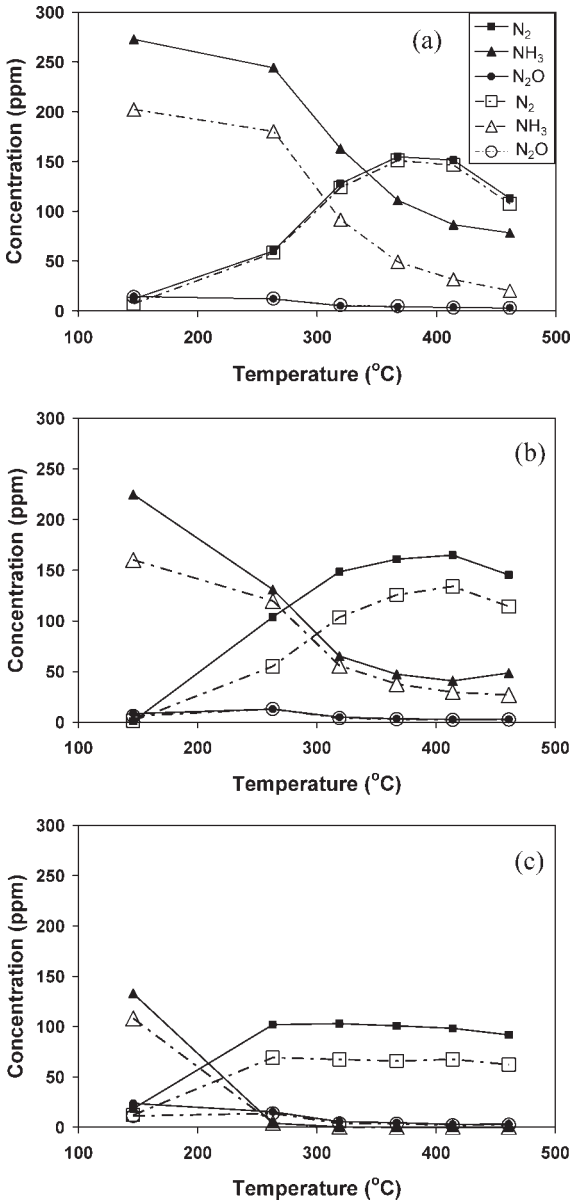

Figure 9. Cycle-averaged results as a function of temperature (---) 0 ppm NO and (—) 500 ppm NO in the rich cycle, catalyst B2.

(a) $S_{N,p}$ = 0.6 (5.1% or 5.0% H_2); (b) $S_{N,p}$ = 0.8 (3.82% or 3.77% H_2); (c) $S_{N,p}$ = 0.9 (3.39% or 3.33% H_2); (Lean: 500 ppm NO, 5% O_2, balance N_2 (60 s); Rich: 1.5% O_2, varied H_2, balance N_2 (10 s)). The legend applies to all three figures.

Additional experiments were conducted to study the formation of N_2 and N_2O during the storage step by cycling between lean (500 ppm NO and 5% O_2) and rich (1500 ppm H_2, t_R = 60 s) until a cyclic steady-state was reached. The formation of N_2 and N_2O during the last lean step was compared with and without NO in the feed (Figure 11). The data showed little difference between the total amount of N_2 produced for the two experiments (Figure 11a). The results suggest that the formation of N_2 during the storage step is mainly caused by NHx species or NH_3 adsorbed on the cata-

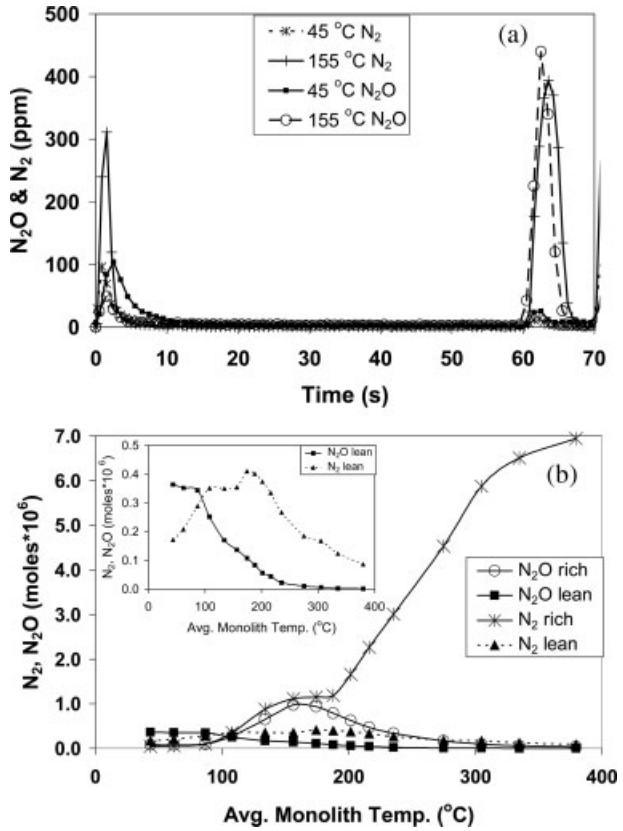

Figure 10. (a) N_2 and N_2O effluent profiles at $T_{M,Avg}$ = 45 and 155°C; (b) moles of N_2 and N_2O formed during the lean and rich steps vs. temperature for monolith B2.

(L = 2 cm) at $T_{M,Avg}$ = 45–380°C (Lean: 500 ppm NO and 5% O_2, balance Ar (60 s); Rich: 2% H_2 and 0.5% O_2, balance Ar (10 s)).

lyst surface, which react predominantly with O_2 during the initial part of the storage step. On the other hand, significantly more N_2O is formed when NO is present during the storage step (Figure 11b). This suggests reaction between gas phase NO and NH_x species that is selective to N_aO formation. The amount of NO fed ($3.7*10^{-7}$ mol/s) during the storage that was reduced during the entire storage step was estimated to be $2.8*10^{-7}$ moles (Figure 11), which is less than the amount of NOx fed in 1 s of the storage.

Analysis and Discussion

The storage data reported in this study are consistent with findings from previous studies but are needed to interpret some of the reduction results. By the end of the rich pulse with H_2 as the reductant, the barium storage sites that are regenerated are in the form of BaO and $Ba(OH)_2$. As the storage step proceeds, NOx is stored in close proximity to Pt[19,24,25] as nitrites and nitrates. Once these sites are filled, the main route to NOx storage is through the disproportionation mechanism.[19,26–31] Kabin et al.[19] proposed that three reaction pathways may occur during NOx storage on Pt/Ba catalysts. The first is for the formation of nitrites and the other two are the routes to nitrate formation.

The initial efficient storage of NOx (with no NOx breakthrough) at low temperatures (150°C) is likely due to the spillover of NOx from Pt forming nitrites on barium and aluminum oxide storage sites. Once the sites in close proximity to Pt are saturated, the major route to NOx storage is through the disproportionation mechanism,[19,26–31] which requires NO_2 transported along the surface or through the gas phase. As NO oxidation is kinetically limited at low to moderate temperatures[29] and occurs negligibly below 150°C, the efficient storage of NOx at the beginning of the lean step diminishes quickly once the proximal sites are filled (Figure 2a). It is noteworthy that the NOx that breaks through at temperatures below 150°C is devoid of NO_2. This suggests that the small amount of NO_2 that is produced from the NO oxidation reaction on Pt at 150°C is efficiently stored.

The storage experiments in which NOx uptake was measured as a function of storage time and temperature revealed the existences of two maxima. One occurs at about 170°C and the other at about 250°C. The more pronounced NOx storage maximum at higher temperature is attributed to the BaO component, while the lower temperature maximum is

Table 2. Percent of N_2 and N_2O Formed During the Lean and Rich; [Lean: 500 ppm NO, 5% O_2, balance Ar (60 s); Rich: 2% H_2 and 0.5% O_2, balance Ar (10 s)]

$T_{m,Avg}$ (°C)	% N_2O Rich	% N_2O Storage	% N_2 Rich	% N_2 Storage	% N_2 and N_2O Rich	% N_2 and N_2O Storage	N_2O Selectivity Storage (%)	N_2 Selectivity Storage (%)
45	18.5	81.5	19.2	80.8	18.7	81.3	67.9	32.1
60	17.8	82.2	21.5	78.5	19.2	80.8	62.8	37.2
85	21.1	78.9	24.6	75.4	22.7	77.3	54.3	45.7
110	52.8	47.2	50.0	50.0	51.2	48.8	41.8	58.2
135	79.1	20.9	71.5	28.5	74.5	25.5	32.8	67.2
155	87.7	12.3	75.8	24.2	80.9	19.1	27.8	72.2
175	89.7	10.3	73.7	26.3	80.1	19.9	20.7	79.3
190	90.4	9.6	74.8	25.2	80.3	19.7	17.2	82.8
200	91.8	8.2	81.6	18.4	84.1	15.9	13.1	86.9
215	91.4	8.6	87.1	12.9	87.8	12.2	11.7	88.3
235	93.8	6.2	91.8	8.2	92.0	8.0	7.8	92.2
275	94.3	5.7	96.1	3.9	96.0	4.0	5.2	94.8
305	93.9	6.1	97.2	2.8	97.2	2.8	3.5	96.5
335	96.2	3.8	98.1	1.9	98.1	1.9	1.8	98.2
380	96.0	4.0	98.8	1.2	98.8	1.2	1.7	98.3

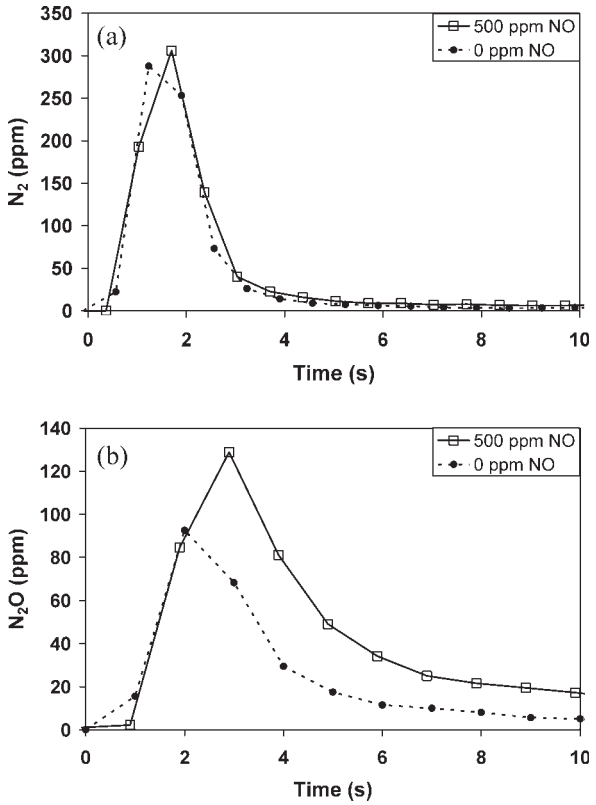

Figure 11. Cycling experiments at $T_{f,inert}$ = 140°C with and without NO in the last lean step, catalyst B2; (a) N_2; (b) N_2O; (Lean: 500 ppm NO, 5% O_2, balance Ar (60 s); Rich: 1500 ppm H_2, balance Ar (60 s)).

attributed to storage on γ-Al_2O_3. Independent experiments with the Pt/Al_2O_3 monolith (Figure 1b) indeed showed that only one maximum in NOx storage occurred at ~200°C. This confirms that the lower temperature maximum on $Pt/BaO/Al_2O_3$ is due in part to the storage of NOx on Al_2O_3. These finding are consistent with those of Lindholm et al.,[22] who observed a maximum in NOx storage on a Pt/Al_2O_3 catalyst at 200°C. As the storage experiments were preconditioned by cycling before each storage experiment was performed, kinetic limitations of the regeneration may affect the amount of NOx stored, especially at lower temperatures. The storage results in Figure 1 therefore represent an effective storage because the catalyst is not completely regenerated prior to the storage experiment. Because H_2 was used as the reductant during the regeneration, which produces a large amount of H_2O, the effects of the kinetic limitations of regeneration on the storage of NOx on Al_2O_3 are probably less than on BaO. This is due to the competitive adsorption of H_2O on Al_2O_3, which is less pronounced on BaO. Finally, in data not shown here, the same $Pt(2.63\%)/Al_2O_3$ monolith catalyst was studied under cycling conditions and was only able to achieve NOx conversions comparable to the $Pt/BaO/Al_2O_3$ catalyst below 100°C (with H_2 as reductant and with other conditions the same). This result supports the concept that γ-Al_2O_3 serves as a storage component at low temperatures and that the γ-Al_2O_3 has a poor trapping efficiency at higher temperatures. Olsson et al.[32] have shown that the addition of H_2O and CO_2 to the storage feed reduces the storage of NO_2 at lower temperatures.

We now summarize a phenomenological picture of the regeneration step of $Pt/BaO/Al_2O_3$ with H_2 as this is essential in understanding the data from this study. On a switch from storage to regeneration, H_2 reacts first with oxygen adatoms, forming water and freeing up sites for stored NOx to be reduced on Pt. The regeneration of the NOx trap is initially limited by the feed rate of H_2. As H_2 flows through the channel, it is consumed rapidly, creating a moving front along the monolith length.[5] Regeneration proceeds from front to back.[5,33,34] Once the H_2 front reaches the end of the monolith and breaks through, NH_3 is observed in the effluent nearly simultaneously (for an anaerobic, dry feed $T > 180$°C).[5] Reactor profiling data reveal that NH_3 is formed upstream and within the H_2 front from the catalytic reaction between hydrogen and nitrogen adatoms, the latter of which are supplied from the spillover and decomposition of the stored NOx. Once NH_3 is formed and desorbs from Pt, it can readsorb downstream and react with stored NOx, Pt-O, or O_2 (aerobic regeneration), as long as the temperature of the monolith exceeds the light-off temperature of the Pt-catalyzed oxidation of NH_3 with NO or O adatoms. The experimental results suggest the following reaction network:

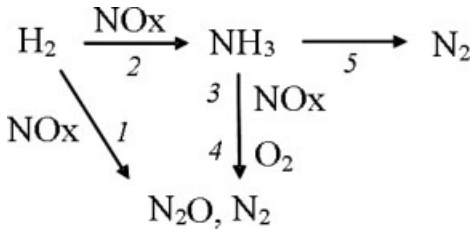

Paths 1 and 2 involve reaction between reductant H_2 and stored NOx to mostly N_2 and some N_2O (path 1) and to NH_3 (path 2). Once NH_3 is formed it can act as a reactive intermediate product; by reacting with stored NOx, forming mostly N_2 (path 3), and with O_2 fed during the regeneration or Pt-O from the previous storage step (path 4), forming mostly N_2. Lastly, the NH_3 can decompose to form N_2 (path 5). The two primary ones are paths 1 and 2. Similarly, N_2O can be produced by the direct and indirect routes. Once H_2 breaks through, the limiting step switches from a feed-limited state to one in which the supply of NOx from the storage phase to Pt is limiting, selectively producing NH_3.

The data in Figures 10b and 11 reveal interesting findings that on switching to the lean feed, N_2 and N_2O briefly appear in the effluent. Breen et al.[35] also observed two N_2 peaks in a single storage-reduction cycle. However, they did not observe the second peak in N_2O during the storage since N_2O is not formed at higher temperatures (350°C). Above 300°C (Figure 10a inset), only N_2 was observed to be produced during the beginning of the storage. The N_2 and N_2O peaks during the storage are more prominent at low temperatures. As the catalyst temperature was increased above 190°C, both of the intensities decreased (Figure 10). The experiments showed that the main cause for the formation of

N_2 and N_2O during the lean feed is due to NH_3 and/or NHx species that are retained on the catalyst during the rich regeneration. As Figure 10 shows, as the catalyst temperature is increased above about 135°C both the N_2 and N_2O peaks decrease in magnitude due to an increased rate of NH_3 desorption; that is, less NH_3 is on the surface of the catalyst at the end of the regeneration. NH_3 desorption experiments were carried out in which a mixture containing NH_3 (400 ppm) in Ar with and without H_2O (1%) was fed to a prereduced catalyst.[20] The results showed that 1% H_2O inhibited the adsorption of NH_3. The results in Figure 11 also confirm that the NH_X species (NH_3) on the catalyst surface are oxidized predominantly by O_2 and to a lesser extent by NO (O_2/NO = 100 in the lean feed). Breen et al.[35] attribute the formation of N_2 during the storage to NH_3 stored on the catalyst reacting with stored NOx, gas phase NOx or O_2. However, our results do not agree with stored NOx playing a role in the formation of N_2 and N_2O during the storage. Similar experiments to Figure 11 were conducted except that the last lean phase consisted of Ar only.[20] For these experiments, N_2 and N_2O were not observed even though stored NOx was still present on the catalyst. In Figures 11a,b, at a fixed temperature (140°C) the N_2O produced increased in the presence of NO, while the effluent N_2 remained approximately constant. This suggests that the NO that is reduced during the beginning of the storage is highly selective to N_2O while the NHx species produced a mixture of N_2 and N_2O, with approximately twice as much N_2 as N_2O. The NOx that reacts at the beginning of the storage is not taken into account in Eq. 1 and thus, the amount of NOx stored will be slightly over estimated at low temperatures. Indeed, the results in Table 2 and Figure 10b show that below 110°C, most of the N_2 and N_2O formed occurs during the storage rather than the regeneration. N_2O formation during the storage is favorable at the lowest temperatures with the selectivity shifting to N_2 formation as the temperature was increases.

Many groups have reported that the NH_3 breakthrough typically coincides with the breakthrough of reductant such as H_2[5,36] and CO.[37] Cant et al.[38] reported that NH_3 is evident only after H_2 breakthrough. However, inconsistencies are reported with respect to H_2 and NH_3 breakthrough times. For example, Nova et al.[36,39,40] have shown that NH_3 breaks through prior to H_2,[40] approximately the same time as H_2,[36] and after H_2 breakthrough[39] for the same conditions (NO/O_2 adsorption, followed by reduction with 2000 ppm H_2, T = 350°C). This may be due in part to anomalous NH_3 adsorption upstream of the analyzer. This underscores the importance of minimizing NH_3 adsorption in the effluent lines and accurately applying time delays if species are monitored by different analytical instruments; for example, H_2 measured by QMS and NH_3 by FTIR. At low temperatures (<160°C), the NH_3 peak is larger than at higher temperatures, which was shown by Clayton et al.[5] to be due to the slow rate of NH_3 reduction of stored NOx and oxidation by O_2 (kinetic limitation) by a systematic variation of the monolith length. As the length of the monolith was increased, the net NH_3 produced increased for low temperatures and remained approximately constant for temperatures exceeding 200°C. Further, Clayton et al.[41] showed that under steady-state conditions the light-off of NH_3 occurred above 180°C with both O_2 and NO as oxidants. However, NH_3 can react below the light-off temperature depending on the Pt surface coverage (to be published elsewhere). NHx species are observed reacting below 180°C during the storage in Figures 2a, 10, and 11.

The data obtained during a 60-s storage on the Pt/BaO monolith (Figure 1a) exhibits a similar dependence on temperature as the NOx conversion (Figures 3a and 4a). This correspondence between NOx conversion and storage shows the effectiveness of stored NOx reduction. That is, once NOx is trapped, hydrogen is very effective in reducing NOx to a mixture of N_2, NH_3, and N_2O. Even at low temperatures, the reduction of stored NOx with H_2 is very effective, exceeding 70%.

A maximum in the selectivity to N_2 occurs at slightly higher temperatures than the maximum in NOx conversion (Figure 3a and 4a). For temperatures above 390°C, the N_2 selectivity decreases while the NH_3 selectivity increases. Interestingly, this is the opposite trend observed for a rich feed under steady-state aerobic[41] or anaerobic[42] NO reduction by H_2. The increasing NH_3 and decreasing N_2 selectivity trends above 390°C are counterintuitive because one would expect the selectivity of N_2 to increase above 390°C due to the increased rate of NH_3 decomposition. For example, at temperatures exceeding 350°C under steady-state conditions NH_3 was shown to decompose.[41] However, Clayton et al.[41] also showed that small amounts of H_2 inhibit NH_3 decomposition under steady-state conditions. Under steady-state conditions, the monolith is exposed to rich conditions throughout, whereas under cycling conditions the monolith is only exposed to rich (reducing) conditions upstream of the H_2 front and within the H_2 front. This suggests that NH_3 will not substantially decompose under these cycling conditions due to the excess H_2 present after H_2 breaks through.

To expand on this issue, it is revealing to analyze the cycling data in the form of cycle-averaged outlet concentration (Figures 3b and 4b). In this form it is evident that the net amount of NH_3 produced is maximum at low temperatures (< 200°C) and monotonically decreases with increasing temperature (Figure 3b). The calculated cycle-averaged N_2 concentration exhibits a similar trend to the NOx conversion (Figures 3a and 4a) and NOx storage (Figure 1a, 60 s). At about 360°C the amount of N_2 produced exhibits a maximum, which coincides with the end of the broad maximum in NOx conversion. At this point, both the net production of NH_3 and N_2 decrease due to the sharp fall off in NOx conversion above 360°C. Thus, the increase in NH_3 selectivity and decrease in N_2 selectivity above 390°C are a result of the different relative rates of decrease in the net NH_3 and N_2 production (Figures 3b and 4b) and NOx conversion (Figures 3a and 4a). As the rate of N_2 formation decreases faster than the net rate of NH_3 formed, the N_2 selectivity decreases while the NH_3 selectivity increases (as there are no other major products formed at these temperatures). A key factor determining the consumption of ammonia is the amount of stored NOx downstream in the reactor. The NOx storage is a decreasing function of temperature in this range, so less stored NOx is available to react with ammonia. Another factor is the presence of gas phase NO during the regeneration step.

The results of Figures 3 and 4 suggest that the regeneration product distribution is sensitive to the amount of NOx stored for a fixed pulse composition and to a lesser extent by temperatures above 200°C. Data obtained at a fixed tempera-

ture and varied amounts of initial NOx stored (Figure 6a,b) show an increase in the N_2 selectivity and a decrease in the NH_3 selectivity as the amount of NOx stored is increased. These trends agree with those of Figures 3 and 4 with respect to the amount of NOx stored. For example, as the amount of NOx stored increases, the selectivity to N_2 increases (see Figure 6a: $T_{M,avg} = 295°C$, Figures 3a and 4a: $T_{M,avg} = 200$ to 275°C and 400 to 530°C). Furthermore, as the amount of NOx stored increases, the speed of the H_2 and NH_3 moving fronts decrease and the time for H_2 and NH_3 breakthrough increases,[5] which is seen in Figure 5a for the NH_3 breakthrough. Clayton et al.[5] showed that prior to reductant breakthrough, N_2 is the primary product formed. So, as the time for the reductant to breakthrough increases (increased NOx storage), the selectivity to N_2 will increase due to the selective reduction of stored NOx to N_2. The N_2 is formed from the direct (H_2 + NOx) and indirect route of NH_3 formation (from H_2 and NOx) and reaction downstream with stored NOx or adsorbed O. Once the reductant (H_2) breaks through, the production of N_2 decreases and the net production of NH_3 increases due to the presence of H_2 throughout the monolith. The high surface coverage of Hydrogen on Pt throughout the monolith inhibits NH_3 from reacting with stored NOx. After NH_3 breaks through a maximum in the net production of NH_3 occurs due to the depletion of stored NOx that is accessible for reaction. The cause for the decrease in NOx conversion with increased lean time is due to increased amounts of NOx breaking through during the storage.

The trends in N_2O reveal different behavior than that of N_2 and NH_3. As the amount of stored NOx is increased, the production of N_2O formed increases up to 60 s of storage (Figure 5b); beyond this point, with further increases in storage time, the difference in N_2O formation are negligible. At the beginning of the pulse, N_2O is predominantly formed by the reaction between adsorbed NO and N, the latter of which is formed by NO bond scission.[19,41] However, N_2O may also be produced from the reaction of NH_3 with stored NOx, Pt-O (from the storage step), or O_2 or NO in the rich feed. The results of Figure 5b show a negligible increase in N_2O formation with increase in lean times (NOx stored) greater than 60 s. This suggests that N_2O formed at the beginning of the regeneration may be attributed to barium storage sites that are in close proximity to Pt that become saturated with NOx during the 60 s of storage. Further, the small change in N_2O with increases in the duration of the regeneration (Figure 7a) also suggests that the initial stored NOx spilling over to proximal Pt sites are selective to N_2O.

The selectivity of stored NOx and gas phase NO fed during the regeneration to products N_2, N_2O, and NH_3 are affected by the pulse composition ($S_{N,p}$), temperature (< 200°C), and amount of stored NOx (Figure 9). The differences between the two N_2 effluent concentration curves and the two NH_3 effluent concentration curves (Figures 9a–c) are attributed to the reduction of the gas phase NO fed to the reactor during the rich pulse. As the pulse becomes less rich ($S_{N,p}$ increased from 0.6 to 0.9), the difference in the net amount of NH_3 formed decreases and N_2 formed increases with and without NO in the regeneration feed. For $S_{N,p} = 0.9$ (Figure 9c), the net amount of NH_3 formed approaches zero at 320°C and was not even observed in the effluent as the temperature was increased to 470°C. As reductant breakthrough did not occur above 320°C, the NOx conversions were insufficient and the catalyst was not nearly as regenerated (especially at the back end of the monolith as the H_2 front did not reach there) when compared with the richer pulse experiments ($S_{N,p} = 0.6$ and 0.8) in which reductant breakthrough was observed.

The main difference between reactions of gas phase NO and stored NOx during the regeneration is likely one of proximity. Stored NOx in the vicinity of Pt will react at the Pt/Ba interface through a spillover mechanism. On the other hand, gas phase NO can adsorb on Pt sites either at the Pt/Ba interface or on Pt sites removed from the interface. Medhekar et al.[43] proposed from the results of TAP studies that two distinct reduction sites exist on the Pt crystallites on the supported catalyst. They speculated that the Pt sites located further from the Pt/Ba interface is where H_2 scavenging of surface oxygen provides a clean surface for NO decomposition to N_2 and N hydrogenation to NH_3. On the other hand, at the Pt sites located close to the Pt/BaO interface, H_2 oxidation, nitrate decomposition, and NO decomposition and reduction occur, producing a complex mixture of N_2, N_2O, and NH_3 which depends on the temperature and effective local NOx/H ratio. Another difference between the two types of NOx is the location along the monolith where the NOx is reduced. The stored NOx will primarily react at the leading edge of the H_2 front; although the NOx stored far from the Pt/BaO interface are reduced more slowly and will react upstream of the leading edge. Similarly, NO fed during the regeneration will react upstream and at the leading edge of the H_2 front, However, as the H_2 front travels through the monolith, the fraction of regenerated monolith increases allowing more gaseous NO fed to react with H_2 upstream. This reaction will selectively produce NH_3 which can then react downstream. Finally, there is a difference between the time when the stored NOx and gaseous NO fed react during the regeneration. Upon the breakthrough of H_2, most of the stored NOx will have reacted it. The temperature exceeds about 230°C. At this point, the dominant reaction chemistry will be between gas phase NO and H_2, until the regeneration is stopped. If the regeneration is excessively long (H_2 breaks through early), the NO fed during the regeneration will cause the NH_3 selectivity to increase with increasing regeneration time, approaching the steady-state selectivity as $t_R \rightarrow \infty$.

At low temperatures (<150°C, Figures 9a–c) the difference in the net NH_3 production with and without NO in the rich pulse is largest due to the reduced rate of NH_3 reacting with stored NOx or adsorbed oxygen. The integral amount of NOx stored is also the least at 150°C. This enables the H_2 front to propagate through the monolith faster[5] causing all of the NO fed during the remainder of the regeneration to primarily form NH_3 (Excess H_2/NO = 40, 15.4, 7). The NH_3 produced from NO fed during the regeneration is observed to react negligibly with O_2 in the feed for $S_{N,p} = 0.6$ (T = 150–460°C); this is based on the increase in the cycle-averaged net NH_3 production of ~60–69 ppm (>85% selectivity of inlet NO fed to NH_3) when NO is fed during the regeneration. The corresponding selectivity of stored NOx to NH_3 was temperature dependent and varied from 5 to 55%. The high selectivity of inlet NO fed to NH_3 is in line with

steady-state results which showed that H_2 is much more reactive with NO than NH_3 under rich conditions.[41] For example, if all 500 ppm of NO fed during the regeneration were converted to NH_3 by H_2 on Pt, the difference in the cycle-averaged net NH_3 observed in the effluent would be 71 ppm ([NO]* t_R/t_{R+S} = (500 ppm) * (10 s)/(70 s) ~71 ppm, where t_R is the regeneration time and t_{R+S} is the total cycle time). Clayton et al.[41] showed that the $NO/H_2/O_2$ system under steady-state conditions attained 100% NOx conversion and produced 100% NH_3 above 200°C for $S_N \leq 0.9$. For the steady-state rich conditions, the Pt surface would mostly comprise H adatoms. However, the Pt surface coverage prior to regeneration is Pt-O and during the regeneration, Pt is also covered by oxygen adatoms downstream of the H_2 front. On the other hand, upstream of the H_2 front, the Pt surface will be predominantly covered by hydrogen and NHx adspecies. Once H_2 breaks through, the Pt surface will be covered by hydrogen and NHx species throughout the monolith. With rich conditions throughout the monolith, NH_3 decomposition is inhibited by the high surface coverage of hydrogen and is unable to further react with stored NOx or O_2 during the regeneration due to the depletion of stored NOx and rich conditions throughout the monolith.

Conclusions

The main contribution of this article is to report and explain performance trends of a model $Pt/BaO/Al_2O_3$ NOx storage and reduction monolith catalyst on several important operating parameters, including the durations of the regeneration and storage times, regeneration feed composition and temperature, and monolith temperature.

The Pt/BaO catalyst exhibits high cycle-averaged NOx conversion above 100°C, with two storage maxima corresponding to NOx stored on the alumina support at lower temperature and BaO at higher temperature. The cycle-averaged selectivities of N_2 and NH_3 on the monolith temperature reveal the role of ammonia as an intermediate that reacts with stored NOx. The duration of the storage is an important determinant of NOx conversion and has a complex effect on the product selectivities. The dependence on regeneration times up to 10 s reveals byproduct N_2O is formed during the first second, while N_2 and NH_3 exhibit a complex dependence that is affected by temperature. Both N_2 and N_2O are formed during the regeneration and storage steps, the latter from the oxidation of NH_x species produced during the regeneration. In some cases, more N_2 and N_2O were produced during the storage step, rather than only during the regeneration, showing the importance of ammonia sorption and reactivity. A comparison of data with and without NO fed during the regeneration reveals a difference in selectivities of gas phase NO and stored NOx. At lower temperature, the selectivities of gas phase NO and stored NOx are similar. However, at higher temperatures, NO fed during the regeneration is more selective to NH_3 than the stored NOx for sufficiently rich regeneration feeds. Three main differences between the reactions of NO fed and NOx stored with H_2 exist causing different product selectivities with varied temperature and H_2 concentration. The differences include the axial location in the monolith, the location on the Pt particle where reaction occurs, and the time when the two types of NOx react during the regeneration.

Although data reported here are for the idealized case of H_2 as the exclusive reductant, these results help to determine how the lean NOx trap can be operated to exhibit high selectivity to N_2 in the case of a conventional LNT, or to NH_3, in the case of a LNT operating in sequence with a SCR reactor. Additional work is needed to understand the role of CO and hydrocarbons in the presence of H_2O and CO_2 which was beyond the scope of this study.

Acknowledgments

The work reported was supported by the U.S. DOE National Energy Technology Laboratory (DE-FC26-05NT42630). The authors also acknowledge BASF Catalysts LLC for providing the catalysts used in this study. This report was prepared as an account of work sponsored by an agency of the United State Government. Neither the United States Government nor any agency thereof, nor any of their employees, makes any warranty, express or implied or assumes any legal liability or responsibility for the accuracy, completeness, or usefulness of any information, apparatus, product, or process disclosed, or represents that its use would not infringe privately owned rights. References herein to any specific commercial product, process, or service by trade name, trademark, manufacturer, or favoring by the United States Government or any agency thereof. The views and opinions of authors expressed herein do not necessarily state or reflect those of the United States Government or any agency thereof.

Notation

F_i = effluent molar flow rate of species i (moles/s).
F_i^0 = feed rate of species i.
$m_{w.c.}$ = mass of the washcoat (g).
S_i = selectivity of species i (%).
$T_{f,inert}$ = feed temperature under inert conditions.
$T_{M,Avg.}$ = average monolith temperature over one complete cycle.
t_S = storage time (s).
t_{S+R} = time for one complete lean and rich cycle (s).
X_i = conversion of species i (%).

Literature Cited

1. Miyoshi T, Matsumoto SI, Katoh K, Tanaka T, Harada J, Takahashi N, Yokota K, Sugiura M, Kasahara K. Development of new concept three-way catalyst for automotive lean-burn engines. *Soc Automot Eng*. 1995;950809:1361–1370.
2. Takahashi N, Shinjoh H, Iijima T, Suzuki T, Yamazaki K, Yokota K, Suzuki H, Miyoshi N, Matsumoto SI, Tanizawa T, Tanaka T, Tateishi S-S, Kasahara K. The new concept 3-way catalyst for automotive lean-burn engine: NOx storage and reduction catalyst. *Catal Today*. 1996;27:63–69.
3. Bogner W, Kramer M, Krutzsch B, Pischinger S, Voigtlander D, Wenninger G, Wirbeleit F, Brogan MS, Brisley RJ, Webster DE. Removal of nitrogen oxides from the exhaust of a lean-tune gasoline engine. *Appl Catal B: Environ*. 1995;7:153–171.
4. Matsumoto SI. DeNOx catalyst for automotive lean-burn engine. *Catal Today*. 1996;29:43–45.
5. Clayton RD, Harold MP, Balakotaiah V. NOx storage and reduction with H_2 on $Pt/BaO/Al_2O_3$ monolith: spatio-temporal resolution of product distribution. *Appl Catal B*. 2008;84:616–630.
6. Kabin KS. NOx *Storage and Reduction Studies on Pt/Ba/Alumina Monolithic Catalysts*. PhD Dissertation. Texas: University of Houston, 2005.
7. Muncrief RL, Kabin KS, Harold MP. NOx storage and reduction with propylene on Pt/BaO/alumina. *AIChE J*. 2004;50:2526–2540.
8. Muncrief RL, Khanna P, Kabin KS, Harold MP. Mechanistic and kinetic studies of NOx storage and reduction on Pt/BaO/Al2O3. *Catal Today*. 2004;98:393–402.

9. Epling WS, Kisinger D, Everest C. NO_X storage/reduction catalyst performance with oxygen in the regeneration phase. *Catal Today*. 2008;136:156–163.
10. Theis J, Jen H-W, McCabe R, Sharma M, Balakotaiah V, Harold MP. Reductive elimination as a mechanism for purging a lean NOx trap. *Soc Automot Eng*. 2006;69–82.
11. Abdulhamid H, Fridell E, Skoglundh M. Influence of the type of reducing agent (H_2, CO, C_3H_6 and C_3H_8) on the reduction of stored NOx in a $Pt/BaO/Al_2O_3$ model catalyst. *Top Catal*. 2004;30/31: 161–168.
12. Mahzoul H, Gilot P, Brilhac JF, Stanmore BR. Reduction of NOx over a NOx-trap catalyst and the regeneration behaviour of adsorbed SO2. *Top Catal*. 2001;16/17:293–298.
13. Liu Z, Anderson JA. Influence of reductant on the thermal stability of stored NOx in $Pt/Ba/Al_2O_3$ NOx storage and reduction traps. *J Catal*. 2004;224:18–27.
14. Abdulhamid H, Dawody J, Fridell E, Skoglundh M. A combined transient in situ FTIR and flow reactor study of NO_X storage and reduction over $M/BaCO_3/Al_2O_3$ (M = Pt, Pd or Rh) catalysts. *J Catal*. 2006;244:169–182.
15. Gandhi HS, Cavataio JV, Hammerle RH, Cheng Y. Catalyst system for the reduction of NOx and NH_3 emissions. 2002. U.S. 7,332,135.B2.
16. Nova I, Lietti L, Forzatti P. Mechanistic aspects of the reduction of stored NOx over Pt-Ba/Al2O3 lean NOx trap systems. *Catal Today*. 2008;136:128–135.
17. Abul-Milh M, Westberg H. Reduction of NO2 stored in a commercial lean NOx trap at low temperatures. *Top Catal*. 2007;42/43:209–214.
18. Ramanathan K, West DH, Balakotaiah V. Optimal design of catalytic converters for minimizing cold-start emissions. *Catal Today*. 2004;98:357–373.
19. Kabin KS, Khanna P, Muncrief RL, Medhekar V, Harold MP. Monolith and TAP reactor studies of NOx storage on $Pt/BaO/Al_2O_3$: elucidating the mechanistic pathways and roles of Pt. *Catal Today*. 2006;114:72–85.
20. Clayton R. Steady-state and cyclic studies of $Pt/BaO/Al_2O_3$ lean NOx traps. PhD Dissertation. Texas: University of Houston, in preparation, 2008.
21. Kabin KS, Muncrief RL, Harold MP. NO_X storage and reduction on a Pt/BaO/alumina monolithic storage catalyst. *Catal Today*. 2004;96: 79–89.
22. Lindholm A, Currier NW, Fridell E, Yezerets A, Olsson L. NOx storage and reduction over Pt based catalysts with hydrogen as the reducing agent. *Appl Catal B*. 2007;75:78–87.
23. Theis JR, Gulari E. Estimating the temperatures of the precious metal sites on a lean NOx trap during oxidation reactions. *Appl Catal B*. 2007;75:39–51.
24. Epling WS, Parks JE, Campbell GC, Yezerets A, Currier NW, Campbell LE. Further evidence of multiple NOx sorption sites on NOx storage/reduction catalysts. *Catal Today*. 2004;96:21–30.
25. Sakamoto Y, Okumura K, Kizaki Y, Matsunaga S, Takahashi N, Shinjoh H. Adsorption and desorption analysis of NOx and SOx on a Pt/Ba thin film model catalyst. *J Catal*. 2006;238:361–368.
26. Scotti A, Nova I, Tronconi E, Castoldi L, Lietti L, Forzatti P. Kinetic study of lean NOx storage over the $Pt-Ba/Al_2O_3$. *Syst Ind Eng Chem Res*. 2004;43:4522–4534.
27. Olsson L, Persson H, Fridell E, Skoglundh M, Andersson B. A kinetic study of NO oxidation and NOx storage on Pt/Al_2O_3 and $Pt/BaO/Al_2O_3$. *J Phys Chem B*. 2001;105:6895–6906.
28. Fridell E, Persson H, Olsson L, Westerberg B, Amberntsson A, Skoglundh M. Model studies of NOx storage and sulphur deactivation of NOx storage catalysts. *Top Catal*. 2001;16/17:133–137.
29. Epling WS, Campbell LE, Yezerets A, Currier NW, Parks IIJE. Overview of the fundamental reactions and degradation mechanisms of NOx storage/reduction catalysts. *Catal Rev*. 2004;46:163–245.
30. Cant NW, Patterson MJ. The storage of nitrogen oxides on alumina-supported barium oxide. *Catal Today*. 2002;73:271–278.
31. Despres J, Koebel M, Krocher O, Elsener M, Wokaun A. Storage of NO2 on BaO/TiO2 and the influence of NO. *Appl Catal B*. 2003;43:389–395.
32. Olsson L, Jozsa P, Nilsson M, Jobson E. Fundamental studies of NOx storage at low temperatures. *Top Catal*. 2007;42/43:95–98.
33. Pihl JA, Parks JE II, Daw CS, Root TW. Product selectivity during regeneration of lean NOx trap catalyst. *SAE Tech Pap*. 2006;2006-01-3441.
34. Cumaranatunge L, Mulla SS, Yezerets A, Currier NW, Delgass WN, Ribeiro FH. Ammonia is a hydrogen carrier in the regeneration of $Pt/BaO/Al_2O_3$ NOx traps with H_2. *J Catal*. 2007;246:29–34.
35. Breen JP, Burch R, Fontaine-Gautrelet C, Hardacre C, Rioche C. Insight into the key aspects of the regeneration process in the NOx storage reduction (NSR) reaction probed using fast transient kinetics coupled with isotopically labelled 15NO over Pt and Rh-containing Ba/Al2O3 catalysts. *Appl Catal B*. 2008;81:150–159.
36. Nova I, Lietti L, Castoldi L, Tronconi E, Forzatti P. New insights in the NOx reduction mechanism with H_2 over $Pt-Ba/g-Al_2O_3$ lean NOx trap catalysts under near-isothermal conditions. *J Catal*. 2006;239:244–254.
37. Epling WS, Yezerets A, Currier NW. The effects of regeneration conditions on NOx and NH3 release from NOx storage/reduction catalysts. *Appl Catal B*. 2007;74:117–129.
38. Cant NW, Liu IOY, Patterson MJ. The effect of proximity between Pt and BaO on uptake, release, and reduction of NOx on storage catalysts. *J Catal*. 2006;243:309–317.
39. Nova I, Castoldi L, Lietti L, Tronconi E, Forzatti P. How to control the selectivity in the reduction of NOx with H_2 over $Pt-Ba/Al_2O_3$ Lean NOx Trap catalysts. *Top Catal*. 2007;42/43:21–25.
40. Nova I, Castoldi L, Lietti L, Tronconi E, Forzatti P. A low temperature pathway operating the reduction of stored nitrates in $Pt-Ba/Al_2O_3$ lean NOx trap systems. *Soc Automot Eng*. 2006:397–406.
41. Clayton R, Harold MP, Balakotaiah V. Selective catalytic reduction of NO by H_2 in O_2 on$Pt/BaO/Al_2O_3$ monolith NOx storage catalysts. *Appl Catal B*. 2008;81:161–181.
42. Xu J, Clayton R, Balakotaiah V, Harold MP. Experimental and microkinetic modeling of steady-state NO reduction by H_2 on $Pt/BaO/Al_2O_3$ monolith catalysts. *Appl Catal B*. 2008;77:395–408.
43. Medhekar V, Balakotaiah V, Harold MP. TAP study of NOx storage and reduction on Pt/Al_2O_3 and $Pt/Ba/Al_2O_3$. *Catal Today*. 2007;121:226–236.

Manuscript received Jun. 16, 2008, and revision received Sept. 1, 2008.